Available online at www.sciencedirect.com
ScienceDirect
Thin Solid Films 516 (2008) 3070–3080
www.elsevier.com/locate/tsf

Tribo-mechanical properties of thin boron coatings deposited on polished cobalt alloy surfaces for orthopedic applications

C.C. Klepper [a,*], J.M. Williams [a], J.J. Truhan Jr. [b,1], J. Qu [c], L. Riester [c], R.C. Hazelton [a], J.J. Moschella [a], P.J. Blau [c], J.P. Anderson [d], O.O. Popoola [d], M.D. Keitz [a]

[a] *HY-Tech Research Corporation, Radford, VA 24141, USA*
[b] *Center for Materials Processing, University of Tennessee, Knoxville, TN 37996, USA*
[c] *Materials Science and Technology Division, Oak Ridge National Laboratory, Oak Ridge, TN 37831, USA*
[d] *Zimmer, Inc, Warsaw, IN 46581, USA*

Received 23 August 2006; received in revised form 24 October 2007; accepted 27 October 2007
Available online 6 November 2007

Abstract

This paper presents experimental evidence that thin (<~200 nm) boron coatings, deposited with a (vacuum) cathodic arc technique on pre-polished Co–Cr–Mo surfaces, could potentially extend the life of metal-on-polymer orthopedic devices using cast Co–Cr–Mo alloy for the metal component. The primary tribological test used a linear, reciprocating pin-on-disc arrangement, with pins made of ultra-high molecular weight polyethylene. The disks were cast Co–Cr–Mo samples that were metallographically polished and then coated with boron at a substrate bias of 500 V and at about 100 °C. The wear tests were carried out in a saline solution to simulate the biological environment. The improvements were manifested by the absence of a detectable wear track scar on the coated metal component, while significant polymer transfer film was detected on the uncoated (control) samples tested under the same conditions. The polymer transfer track was characterized with both profilometry and Rutherford backscattering spectroscopy. Mechanical characterization of the thin films included nano-indentation, as well as additional pin-on-disk tests with a steel ball to demonstrate adhesion, using ultra-high frequency acoustic microscopy to probe for any void occurrence at the coating–substrate interface.

Keywords: Boron; Amorphous materials; Coatings; Biomaterials; Deposition process; Rutherford backscattering spectroscopy; Tribology; Cobalt alloy

1. Introduction

By far the most favored technology for construction of the articulating parts of artificial hips and knees is that of an alloy component (e.g., the spherical head of a hip joint) rubbing against a mating component of ultra-high molecular weight polyethylene (UHMWPE). For several years it has been accepted that one of the biggest, if not the biggest, problem with this technology relates to bone loss (*osteolysis*), which is caused by tissue reaction to wear debris from the UHMWPE. The result can be loosening of the prosthesis within its fixation and ultimate failure. There is now a huge literature to this effect, together with studies of wear, wear mechanisms, and wear prevention ideas for the UHMWPE. Some of this literature will be cited below. The present effort is directed to wear prevention by use of a boron coating for the favored alloy, Cobalt–Chromium–Molybdenum (Co–Cr–Mo).

Co–Cr–Mo alloys are, in fact, the most common materials used nowadays for orthopedic devices for total hip or knee replacement, or, in medical terminology, *total joint arthroplasty* (TJA). In particular, cast Co–Cr–Mo material is used for knee TJA devices, because the complexity of the shape of the knee would prevent any other metal processing technique to be cost-effectively employed. In the casting process, carbide precipitates are known to form; these appear as hard protrusions on the surface after polishing.

Early atomic-force-microscopy topographical studies [1] showed the elevations of the carbides above the matrix surface to be in the range of 15 to 30 nm, with the carbides having mesa-

* Corresponding author. Tel.: +1 540 639 4019; fax: +1 540 639 4027.
E-mail addresses: kleppercc@ieee.org, cklepper@hytechresearch.com (C.C. Klepper).
[1] Presently with Caterpillar, Inc., East Peoria, IL, USA.

0040-6090/$ - see front matter © 2007 Elsevier B.V. All rights reserved.
doi:10.1016/j.tsf.2007.10.111

like shapes with rather sharp edges. The carbides, known as "block" carbides, cover regions of tens of μm wide and hundreds of μm long. The reported hardness values were about 5 GPa for the matrix and about 15 GPa for the carbides [1]. From these hardness values, together with the loose correlation between the spacing of the carbides and the spacing of asperities in conventional profilometry, and the fact that the average roughness (Ra) values in profilometry were in broad agreement with the up-thrust values of the carbides, it seemed apparent that the limit to polishing smoothness was relief polishing due to the difference in hardness between the matrix and the carbides. Moreover, carbide plateaus and alloy matrix valleys, by themselves, had respective Ra values of about 2 nm and 1 nm, respectively. The results were the same for a relatively "hard" polishing compound (diamond) and a relatively "soft" polishing compound (colloidal silica). Thus, the up-thrust of the carbides apparently accounted for all of the deviation of the surface from a potentially optical grade of polish of less than 1 nm in smoothness. Moreover, in laboratory prepared materials, these were the only asperities found of dimension above a background suggested by the smoothness value of about 1 nm.

The mix of wear mechanisms operating in clinical prostheses of the described technology may not be completely clear in terms of quantitative division among possible mechanisms. On the one hand, the UHMWPE components, whether obtained from long term simulator tests or from clinical explants, usually exhibit burnishing or polishing over most of the contact area [2,3]. These burnishing results, for both types of wear exposure, are suggestive of a controlled removal of material in small particles, and in fact, most of the wear debris itself, consisting as it does of submicron particles [2,3], can be construed as supporting the same idea. Furthermore, the forms of the small particles, spheres and fibrils, may not be directly related to the wear mechanism, but instead appear to consist of microspheres and fibrils that were originally part of the UHMWPE structure [4]. At the same time, a difference between the simulator results and the clinical results, is that for the clinical, there are some larger scratches and troughs. These have been attributed to foreign abrasive matter such as bone cement filler or polishing compound that has been left in the alloy surface [2,5]. Another mechanism more recently brought to the fore [2] is that the foreign abrasives scratch the alloy, and then in turn, scratches on the alloy produce wear of the UHMWPE. It is possible that embedding of particles in the UHMWPE, and thence scratching of the alloy surface is a larger effect than the correlated one of embedding particles in the alloy and scratching the UHMWPE. Ref. [2] forms part of a series by the same research team. A different technology, that of zirconium oxide on a zirconium substrate is compared with the Co–Cr–Mo technology, both with and without scratches. The wear rates are different, but the size distribution is the same regardless of base technology. All of this evidence supports the idea that the morphology of the wear debris is essentially a property of the UHMWPE structure rather than being related to details of the wear mechanism.

Only those wear effects that occur in the clean simulator type of test appear intrinsic to the alloy–UHMWPE couple. The others could be improved, in principle, by improved manufacturing techniques or by improved surgical procedure. The hypothesis of the present paper is that the precipitated carbides are likely to be the key factor in intrinsic wear. Specifically, the idea is that the highly articulated microstructure of these up-thrusting carbides might be buffered by a boron coating of a thickness of some ten times the up-thrust and with thermodynamically predicted, good adhesion to the Co–Cr–Mo alloy. Moreover, other properties of the chosen, thin film coating material could also contribute to success of this surface engineering treatment, as will be now discussed.

The choice of (vacuum) cathodic arc-deposited, amorphous boron as the coating material was based on a number of factors:

First, boron (B) is a very hard material. In crystalline form, the hardness is 30 GPa, about three times as hard as silica sand. Recent studies that amorphous boron thin film can be produced with hardness approaching that of crystalline boron, but with a lower elastic modulus [6–12]. In these studies, the reduced modulus, which benefits thin film coatings by increasing the impact resistance, is attributed to a very small, but often unavoidable, oxygen incorporation in the coating.

The high hardness, which could then be provided by the amorphous boron coating, would provide an additional benefit for TJA devices. It would help protect the metal surface from damage when hard particles, typically from bone debris and fixation cement, get caught between the polymer and the metal surface. Furthermore, the choice of an amorphous coating material removes the concern about variations in crystalline structure depending on whether the deposition is on a carbide-rich or carbide-free region of the substrate surface.

Second, boron is known to have highly favorable heats of mixing with most transition metals, including titanium, the components of the cobalt alloy and that of most steels. The results of thermodynamic calculations for Co, Ti and Fe are given in Ref. [13] and they show maximum negative values for the enthalpy of mixing of 34, 38 and 84 kJ/mol of total atoms, corresponding. These high heats of mixing foretell the probability of reaction of B with the substrate. Reaction modes could include compound formation, as is indicated by many binary phase diagrams of transition metals, or possible in-diffusion, if for some reasons the compounds do not nucleate. Since concern about delamination is the main reason that metallurgical coatings are generally avoided in TJA applications, great attention must be paid to adhesion. The combination of the favorable thermodynamics, the small size of the boron atom, which may better allow diffusion into the substrate, and the energetic ion deposition characteristic of cathodic arc deposition, are all favorable indicators for cathodic arc-deposited boron films with reaction bonding to the substrate.

A third reason to consider boron is that, in a moisture-containing environment, its surface oxide is known to form a hydroxide layer, which acts as a solid lubricant [14]. The reaction involved is

$$1/2B_2O_3 + 3/2H_2O \rightarrow H_3BO_3$$

$$\Delta H_{298K} = -45.1 \text{kJ/mol}$$

The lubricity of boric acid has been attributed to its tendency to form a triclinic crystal structure made up of atomic layers

parallel to the basal plane. In each layer, the B, O and H atoms are closely packed and bonded to each other with mostly covalent bonds, while the layers are held together with the weaker van der Waals' forces [14]. It is the freedom of the layers to slide with respect to each other that produces the lubricity in this model.

Finally, a crucially important reason for this choice of coating material was the expectation that boron would be biocompatible. This expectation was based on the very high resistance of boron to attack by halides [15], since the resistance to release of ions due to salt corrosion in the body is one key element of biocompatibility. Moreover, ion release from boron, when it occurs, is expected to be in the form of boric acid, which is a mild antiseptic, commonly used in ophthalmic solutions. The results of a recent, standardized biocompatibility study of boron, and boron-coated Co–Cr–Mo are consistent with these expectations, and will be reported separately from this paper [16].

The aim of the present paper is to describe the results of the coating experiments and the evaluation of the mechanical and wear properties of the resulting coatings with regard to their suitability for this socio-economically important orthopedic application. Since the use of amorphous boron and boron sub-oxides thin films in surface engineering, and the use of the vacuum cathodic arc technique to apply these thin films, are both emerging technologies, some discussion on the films and the deposition is included in the paper.

2. Experimental details

2.1. Deposition of amorphous boron coatings

The heated-cathode, vacuum cathodic arc process used to deposit boron coatings from a sintered pure boron cathode is described elsewhere [8,13,17]. The important, most recent development in this coating technology is the use of a new filter [13,17], which is very effective in removing particulate contamination, typically associated with the cathodic arc process. The filter reduced particulate incorporation to less than 2 particles per cm^2 per 100 nm of deposition. This made it possible to easily find regions totally devoid of particles for the wear test. Optimization of the filter is a continuing effort.

The most important deposition parameters are summarized below:

Cathode: Sintered boron, heated to ~1000 °C
Substrate: Flat coupons of cast/solution annealed ASTM F-75 alloy (also referred to as Co–Cr–Mo or Zimaloy), polished to less than 25 nm (maximum average "Ra" surface roughness value as determined with a Zygo NewView™ 5000 interferometer at Zimmer).
Substrate bias: −500 V with respect to chamber ground and with spark suppression
Substrate heating: About 100 °C with up to 50 °C increase during the deposition
Background gas: None.
Base pressure: About 10^{-4} Pa [$\sim 5\times10^{-7}$ Torr] with the cathode hot
Deposition rate: Typically ~2–3 nm/s (with particle filter)

Substrate preparation at HY-Tech simply involved ultrasonic cleaning in 50% Purple Power™ alkaline cleaner and water for 30 min, followed by water rinse, methanol rinse and blow drying with canned air (i.e., high purity tetrafluoroethane, commercially available in a spray can). Since past experience, with steel samples [18], indicated that the arc plasma is sufficiently effective at removing any intrinsic oxide layers from the substrate surface, no discharge cleaning was deemed necessary for these coating runs.

The mentioned flat samples were coated with boron to thicknesses varying from about 150 nm to as much as 400 nm, in regions clearly distinguishable by the color of the coating. The light coatings have a light blue color, while the thick coatings exhibit a tan color; beyond 500 nm, amorphous boron is essentially grey; crystalline boron would be black. It is noted that even the 150 nm amounts to several times the thickness of the typical carbide protrusion.

2.2. Surface morphology studies

A Hysitron TriboIndenter® was used to characterize the surface morphology of the substrates before and after coating. The apparatus allows for rapid, spatially resolving measurements of the surface topography as well as of the nano-scale hardness and elastic modules. Friction coefficient measurements are also possible, although this capability was not used here. Since the instrument was used primarily for its surface scanning, as well as nano-indentation capabilities, it will be henceforth referred to as a *scanning nano-indenter*.

In spatially scanning mode, the instrument produces two types of output from which the topography can be deduced: (i) It puts out the vertical displacement of the indenter tip as it sweeps across the surface and (ii) it puts out the horizontal force on the tip as a result of encountering a positive or negative slope in the surface. In this way, the protruding carbide features anticipated from the literature could be detected and any impact of the coating in altering the shapes of these protrusions could be observed. In static mode, it was possible to locate the indenter tip on the top of a carbide formation to perform highly localized nano-indentation. This, in turn, can be used to deduce if the peaks of the carbides are coated and if the coating changes the hardness and modulus of the carbides differently that it would in carbide-free regions of the substrate.

2.3. Wear testing

An existing setup designed for reciprocating pin-on-disk motion, with the disk (coated or non-coated sample) moving, while the pin is stationary, was modified to have a reservoir around the sample allowing the sample to be submerged in a saline solution. The setup allowed for selectable static load to be placed on the pin. The existing setup also provided for an automatically recorded coefficient of friction as a function of time during the experiment.

The specially made UHMWPE "pins" were 6-mm diameter rods with hemispherically formed contact ends. The load was

10 N. The traverse was purely linear and cyclic with a 1 s period and a stroke of 6.7 mm. The test duration was 24 h. The immersion medium was saline at 3.5 wt.% NaCl in distilled H_2O. The combined elasto/plastic properties of the pin were such that the contact area under the 10 N load was of approximately 0.8 to 1.0 mm in diameter.

2.4. Compositional characterization of coating and transfer film

Access to an accelerator facility for Rutherford backscattering spectroscopy (RBS) was of great value to this study, because the technique allows for characterization of both the composition and the thickness of coating and interlayer, before using the same sample for a wear test. That is because RBS, together with its companion technique, non-Rutherford elastic scattering (NRES) is a totally non-destructive way of analyzing materials. It is based essentially on the alpha particle elastic scattering experiments that originally provided the basis of the Rutherford nuclear model. The fully stripped helium ions (He^{++}) derived from accelerators have nuclei that are the same as alpha particles, and are still overwhelmingly the favorite incident particle for analysis. The terminology for the two related techniques, both used in the present study, is recalled here:

Rutherford backscattering (RBS)
Elastic nuclear scattering with the cross section of the Rutherford nuclear model derived from the nuclear Coulomb potential.

Non-Rutherford elastic scattering (NRES)
Elastic nuclear scattering, but with an enhanced cross section which may apply over a limited incident particle energy range for certain atoms.

It is also recalled that the Rutherford cross section goes as Z^2 for atoms. Thus, heavy elements are much more detectable than light ones for RBS. As a fortunate counterpoint, for the light elements involved in the coating, favorable NRES reactions are often available at selected energies for light elements.

More details on this well-established, non-destructive technique can be found in Ref. [19]. The best-known simulation code is RUMP [20], which was used for the present analyses. RBS data and NRES data can be mixed in the same yield spectrum, depending on what cross sections actually apply at the given particle energy.

For most of the studies reported below, an energy of 4.27 MeV was used for the incident He ions. This energy produces a sharp resonance for carbon, and is on the lower threshold of a resonance for boron. The detector angle was at 170° relative to the incident ion beam. Thus, the return ions were actually at 10° from being directly backscattered at 180°. This, in any case, is the most common geometry used.

2.5. Adhesion and coating–substrate interface studies

The mentioned pin-on-disk wear tests were aimed at determining the impact of the boron surface-treatment of the cobalt alloy surface on the wear of the polymer counter-surface. To test the strength of the coating–substrate bond (it is recalled that no intermediate bond coating was used in the process) and to demonstrate the durability of the coating, even in the event of accidental third body wear by loose bone or cement particles, a friction/wear test was also carried out using the same test assembly. For this testing, reciprocating ball-on-flat sliding was utilized with a 52100 bearing steel ball (9.5 mm diameter) under a 2 and 10 N load, and lubricated by mineral oil.

The analysis included optical microscopy inspection of the wear track and surface/subsurface examination by use of Scanning Acoustic Microscopy (SAM). A state-of-the-art instrument, a KSI SAM-2000 scanning acoustic microscope, was used for the latter measurement. Frequencies up to 2 GHz are possible with higher frequencies providing for more depth resolution. A model was developed for boron (not originally in the instrument's database) and the measurements were carried out at about 400 MHz. In a material with the low molecular weight of boron, the depth resolution is limited to 0.1–0.3 μm at the interlayer (about 0.2 μm below the surface of the boron top coating). More resolution is possible inside the interlayer, which is dominated by Co (a high molecular weight material). Still, at this resolution, localized delamination should be detectable. The advantage of the instrument is that it can non-destructively detect voids forming at the interface, before delamination actually appears at the surface. As such, it is significantly more sensitive to adhesion problems than the more commonly used scratch testing.

3. Experimental findings

3.1. Morphology and nanohardness of coated surfaces

Fig. 1 shows the surface morphology of a typical (flat coupon, pre-polished, as described in Section 2) substrate, before coating and as determined by the scanning nano-indenter. The carbides are seen to span areas of tens of microns by hundreds of microns on the polished surface consistent with earlier results (e.g. [1]).

Fig. 2 shows the surface morphology of a coated surface. The case shown is from one of the thicker coatings produced in the present study, having a thickness of about 300 nm. The topographies appear similar to those of the non-coated substrate in Fig. 1. Similar sized regions are displayed with similar concentrations of carbide formations; coated and uncoated samples come from the same batch of polished samples. The thinner coatings produced similar topographies as the thicker coatings. Thus, the surface texture seen in these images are not a property of the coating, but rather the substrate template is projected through the coating. This conformal coating can be understood as a result of the very small plasma sheaths that result from the high electron densities (10^{12} cm^{-3} range) and low electron temperatures (few eV) typical of a cathodic arc plasma. Such plasma conditions lead to sheaths comparable or smaller that the lateral dimensions of the carbide features seen in the images.

The coatings are clearly devoid of *macroparticles* [21,22], the micron-size particulates that constitute a common concern

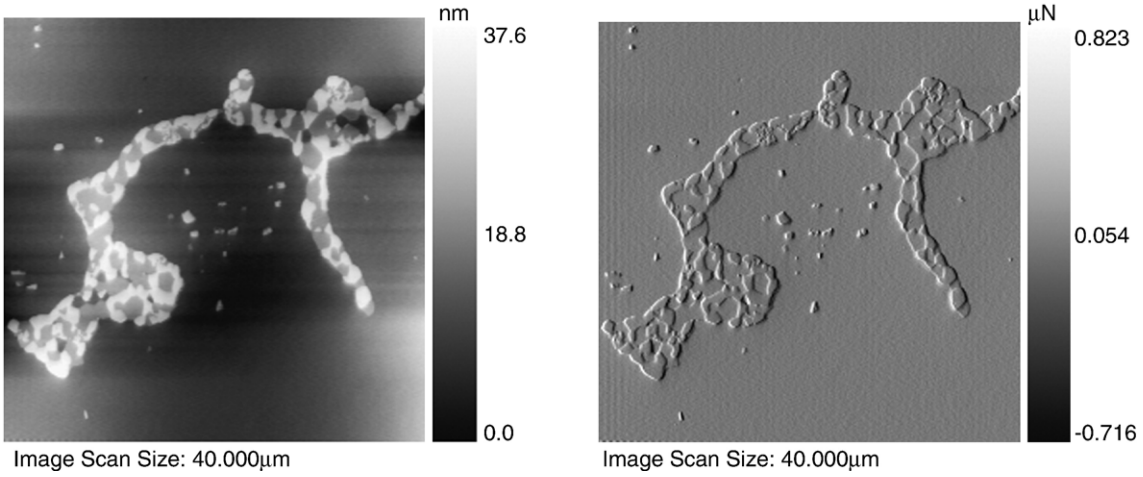

Fig. 1. Surface morphology images of an uncoated, cast/solution annealed, polished Co–Cr–Mo substrate, as produced with the scanning nano-indenter. The image on the left is ~40 µm×40 µm and generated from displacement data. The one on the right is ~10 µm×10 µm and generated from gradient data.

regarding the quality of cathodic arc-deposited coatings. This is a result of the macroparticle filter recently developed and optimized for non-metal cathode applications, where the macroparticles tend to be in solid form and are difficult to filter out with common techniques developed for metal cathodes, which in turn produce liquid phase macroparticles. The filter and its advantages have been discussed elsewhere [13,17].

Of main interest in this study was to determine if the boron coating would smooth out the sharp carbide features, which would in turn reduce the wear of the polymer counter-surface. However, this proved not possible with the scanning nano-indenter. The size of the pyramidal indenter tip (~50 nm at the tip with a face angle of 65.3°, or an equivalent cone angle of 70.32°, thus becoming quite wide with a small penetration into the surface) did not permit a very detailed description of the edges of the mesa structures. As a result, it was very difficult to tell if the abruptness of the edges modified by the coating to any significant extend. Of great value, however, were the micron-scale topographic study of the surface and the measurements of the changes in the hardness as a result of the coating, as will be discussed. With regard to the salient topography, it did not appear to be altered, even with the thickest coatings.

Although the thicker (>~250 nm) coatings did not show any delamination tendency upon indentation, they tended to delaminate in the polymer wear tests in the saline solution. The thinner coatings (<~250 nm) exhibited no delamination in the polymer wear tests, nor in the sliding tests against the steel ball, as will be discussed. Therefore, the rest of the paper will focus only on the thinner coatings.

Regarding the nano-indentation results from the scanning nano-indenter, the tops of the mesas were found to be substantially harder than the regions away from the mesas for the non-coated samples. This was anticipated, since the carbides are known to be very hard compared to the metal alloy. It is known from studies of adherent, thick (>~400 nm) coatings (mostly on bearing steel substrates) that the cathodic arc-deposited, boron coating hardness itself is about 26 GPa and the modulus is about 290 GPa [8]. For the thin (~150–200 nm)

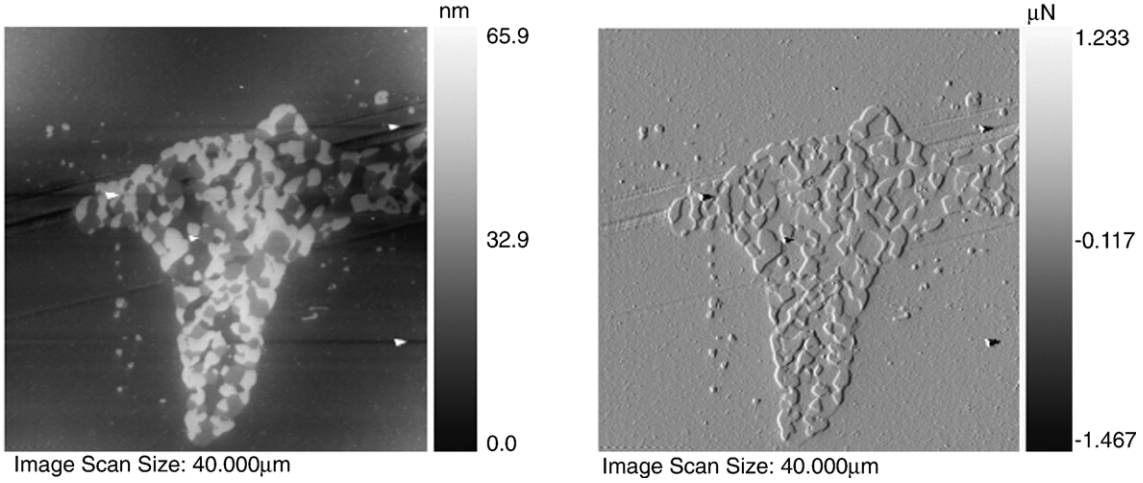

Fig. 2. The surface morphology of a coated surface, on a substrate from the same batch of cast/solution annealed, polished Co–Cr–Mo substrates as that of Fig. 1; images produced with the same technique and same scale.

coatings on the Co–Cr–Mo matrix, the indenter penetrates the coating. The resulting composite hardness was 12.5 GPa, which was about 50% higher than the hardness of the matrix without the coating, and the system modulus was 193 GPa. More interestingly, the hardness of the carbides was reduced from 31.4 to 14.4 GPa and the modulus of the carbides was reduced from 429 GPa to 227 GPa. From the RBS results, to follow in Section 3.3, this can be correlated to some in-diffusion of B into the carbides. Thus, the effect of the coating is somewhat like the effect of ion implantation in making the moduli and the hardness values presented at the surface as more uniform [1].

3.2. Polymer wear test results

The results of these wear tests were as follows. In comparison with uncoated Co–Cr–Mo, the average friction coefficient was reduced by approximately a factor of two for the boron-coated coupon. The averaged values were approximately 0.02 for the uncoated sample and approximately 0.01 for the coated sample. Thus, friction was very low in this submersed environment, as might be expected.

Fig. 3 shows profilometry traces across the wear track on the Co–Cr–Mo disk after a 24-h run. These reveal a transfer film of about 150 nm for the uncoated sample and no detectable change in topography for the coated. RBS analysis of the wear track region of the coated samples confirmed that the thickness of the boron coating remains unchanged; i.e. there is no loss in coating material. The composition of the transfer film and of the coatings, as well as the coating–substrate interface, is discussed in the next section. The result of Fig. 3 was typical of three similar wear tests using UHMWPE pins; a new pin was used for each coated surface. Only one coated sample was selected for the compositional analysis.

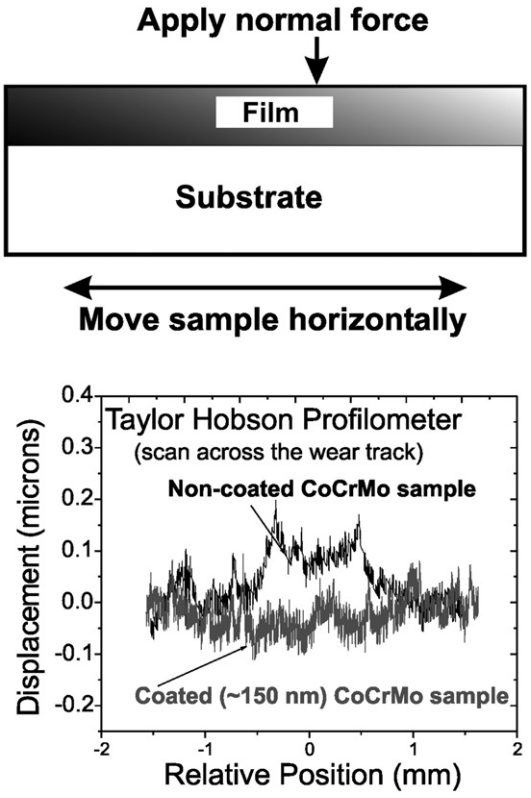

Fig. 3. Traces from profilometry across the wear track for non-coated (black line) and coated (red line) samples, both used as the disk in the reciprocating pin-on-disk tests with UHMWPE pins.

The mass loss on the polymer pins was too small to measure with available scales. Qualitatively, it was possible to observe the difference in wear of the polymer. In the tests on the non-coated samples, visible polymer debris started to accumulate on the surface of the saline solution, even after the first hour of the 24-h tests. Such debris was not detected in the tests performed on the coated samples. Although most of the debris was collected in one of the pin-on-disk runs, it was found to be difficult to measure the mass reliably. This is why the characterization of the wear track, presented in the next section, is of critical importance in supporting the conclusion that the boron coating reduces the wear of the UHMWPE surface. Although the results are mostly qualitative in nature, they were consistently reproduced over three 1-h runs and three 24-h runs. More extensive, longer duration wear studies, using non-linear, bi-directional ("cross-shear") pin motion [23–25], to better simulate hip and knee articulation, are planned for a follow-on study.

3.3. Composition of the deposited films and of the transfer film

Fig. 4 shows an RBS histogram for the base material to use for reference when fitting the data for the coated material. Specifically, it is the analysis of an uncoated area of the Co–Cr–Mo, prepared and polished in the same way as the samples that were coated. A simulation for the best-fit composition of the material is also shown on the graph. Thus, this result is representative of the material without coating and without any exposure to a wear study.

The composition fitting the simulation (in atomic fraction) is: 0.62 Co, 0.35 Cr, 0.03 Mo. In weight fractions these values correspond to: 0.63 Co, 0.32 Cr, 0.05 Mo. These values are slightly different from the normal specifications of the ASTM F 75 alloy in weight fractions: 0.66 Co, 0.28 Cr, 0.06 Mo. The large carbon peak is due to a NRES reaction, and was analyzed as described above. The amount of surface C was 1.5×10^{16} atoms/cm^2 or about 15 atomic layers.

Fig. 5 shows a full-range RBS spectrum of a coated sample to measure and simulate coating thickness and composition. The curve highest in energy is the reference curve of Fig. 4. The other two are for the coated area and the simulation of the coated area. From the simulation (and primarily from the energy setback), the coating thickness is determined to be 180 nm of boron. In addition, there is change in slope for the principle "ledge," that being the rise due to Co. This slope change is detectable for Co because it has only one isotope. As a result any change in the form of the edge due to a reaction layer is more detectable than for the Cr and Mo edges that have several isotopes. It was determined by simulation (RUMP) that the reaction layer, presumably due to in-diffusion or compound formation by the B, was 50 nm thick. Since this layer is still rather thin, it was modeled simply as a composition of 50 at.% B and 50 at.% of the

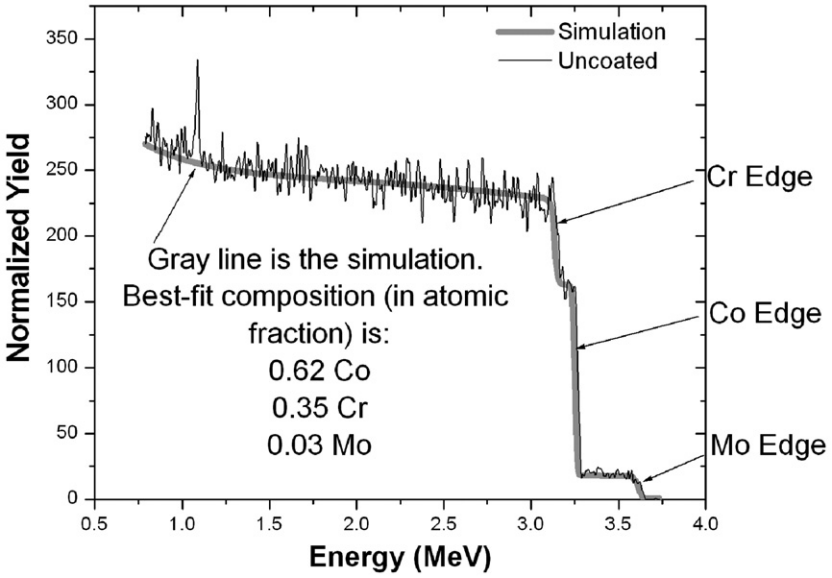

Fig. 4. Full-range RBS spectrum on non-coated sample to measure and simulate substrate composition. A 4.27 MeV He^{++} beam was used as the input. The simulation is also shown.

original alloy constituents in the same proportion as the whole alloy. The coated sample used for this measurement was the same sample as the one used in the wear tests, whose results are shown in Fig. 3. However, the measurement was done away from the wear track. Incident ions were at 4.27 MeV, as stated.

The main conclusion from this result is that this coating was 180 nm including an apparent bonding reaction layer of 50 nm thick, intermixed into the alloy. The range of the ions at the deposition energy of 500 eV is only 2 nm. Hence this result represents a chemical reaction driving the boron inward to some degree. The overall thickness is what was expected from the color (light blue) of the coating and from the ion dosimetry during the arc deposition of the coating. It is recalled that that plasma from a vacuum arc is fully ionized; thus the deposition can be reasonably well monitored by integrating the ion current.

The determination of the coating thickness utilized the upper range of backscattered ion energies in the RBS spectrum of Fig. 4, where the edges of the metal components of the Co alloy substrate are found. Careful examination of the lower range, where the light elements are found, reveals that the carbon peak

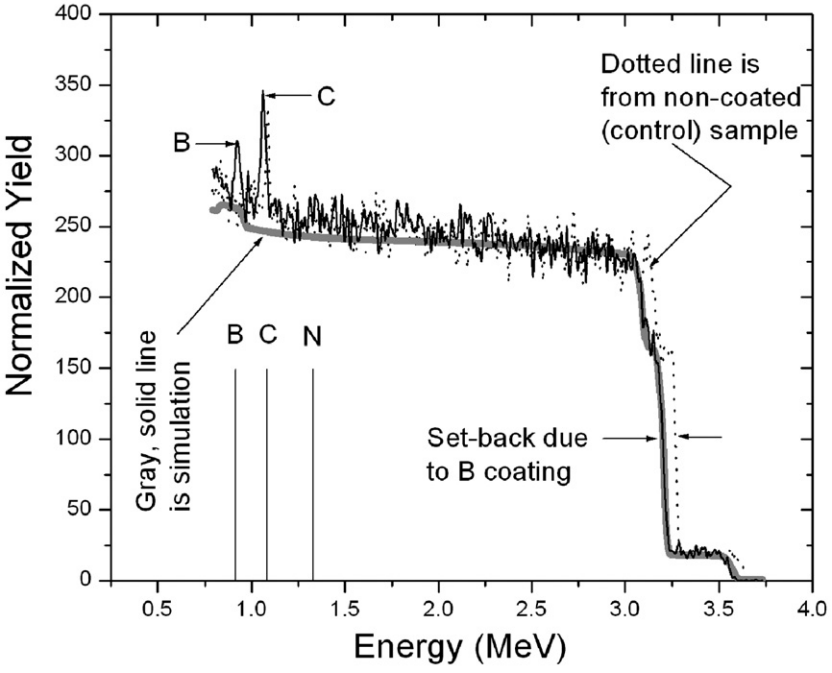

Fig. 5. Full-range RBS spectrum of a coated sample to measure and simulate coating thickness and composition. A 4.27 MeV He^{++} beam was used as the input. The simulation is also shown and the control sample spectrum of Fig. 4 is superimposed for thickness measurement reference.

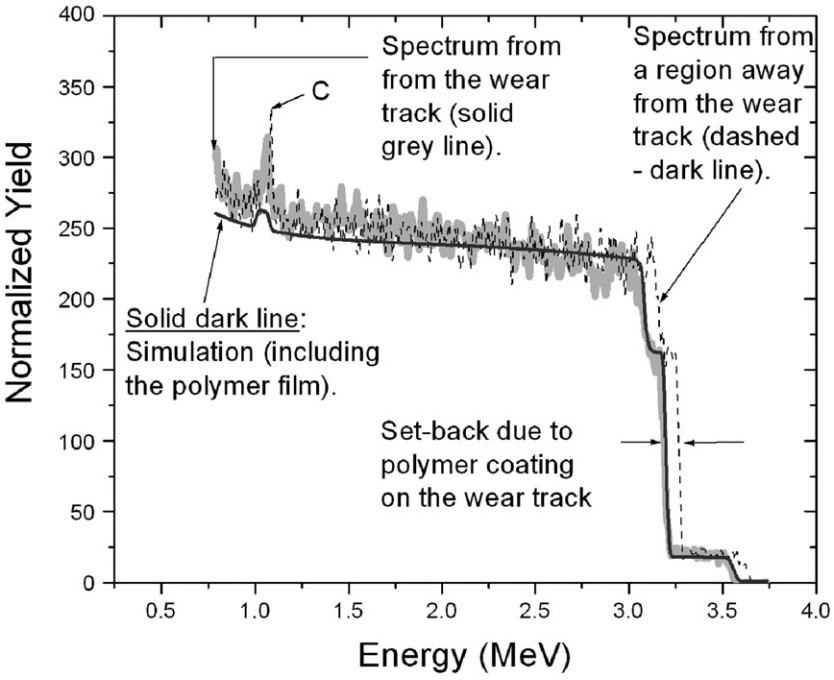

Fig. 6. Full-range RBS spectrum on the wear track, after the UHMWPE pin-on-disk wear test on a non-boron-coated sample, compared with a region away from the wear track on same, non-boron-coated sample. The superimposed simulation includes the composition from Fig. 4 and a model for the polymer transfer film, consistent with Fig. 3.

for the B-coated sample is considerably wider than for the uncoated sample. Furthermore, examination of the histogram to the left of the spectral edge position identified by the "C" marker on the horizontal scale, the carbon remains high as one moves inward from the surface, however the edge of the carbon signature does not shift in the same way (or to the same extent) as the edge of the metal signature. This result means that carbon is in the boron coating and not just on the surface of the substrate. Further analysis of the combined result yields that there is a little over 4 times as much carbon in the B-coated area as in the non-coated area. This amounts to a little over 6×10^{16}/cm^2 of C in the coating.

Expressed as a fraction of the boron atoms in the coating, this would still be only about 2%. Therefore, one can conclude that

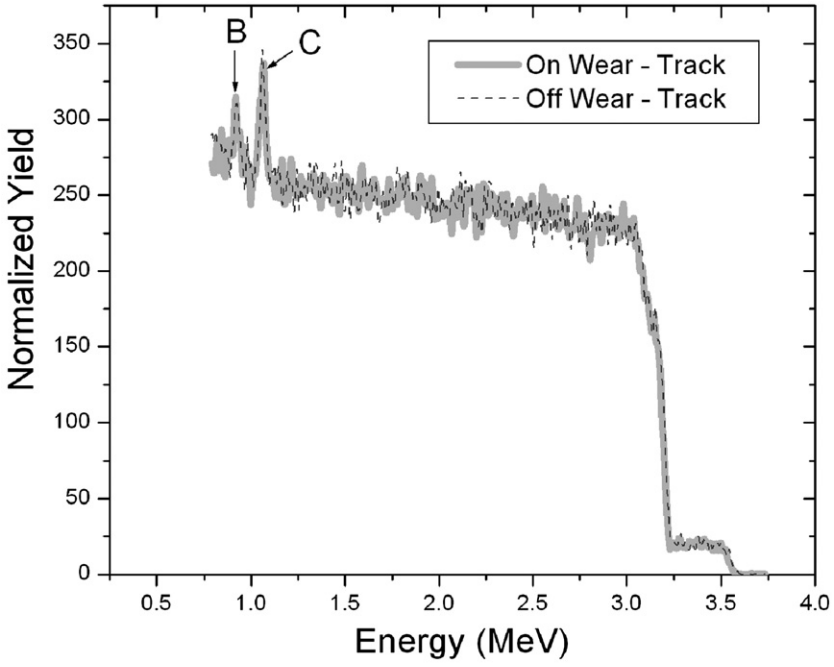

Fig. 7. Full-range RBS spectrum on the wear track, after the UHMWPE pin-on-disk wear test on a boron-coated sample, compared with a region away from the wear track on same, boron-coated sample. The absence of any shift in the edges of the Co, Cr and Mo components of the spectrum imply a total absence of transfer film, consistent with Fig. 3.

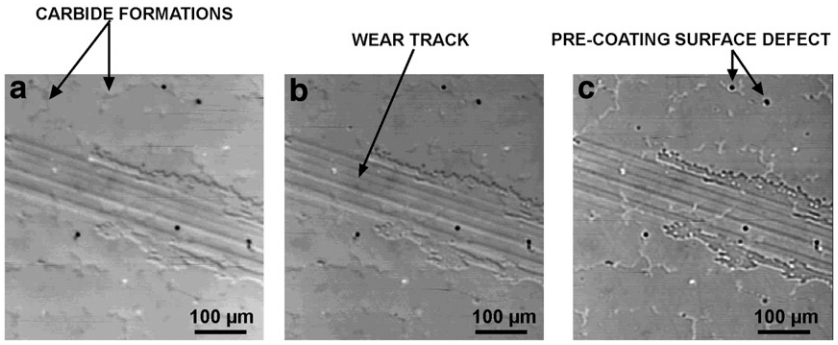

Fig. 8. SAM images of the coated surface tested in sliding motion against a steel ball at a tested at 10 N load. From left to right: (a) surface, (b) subsurface layer $z=0$–2 μm, and (c) subsurface layer $z=2$–4 μm.

the amount of carbon impurity is fairly minimal by the standards of most mechanical coatings. The peak at 0.8 MeV is due to B, where the B is also detectable at that level because of a NRES cross section. That NRES cross section is not as large as the carbon NRES cross section at that energy. Thus, the B peak is smaller and that reaction soon gets out of resonance at still lower energy. The main conclusion here is that the coating contains some carbon but not so much that one need be concerned about impact on adhesion and on the mechanical properties of the coating [8].

Fig. 6 compares RBS spectra from the wear track on the non-coated (control) sample with those from a region clear of the wear track on the same sample. This time the setback in energy on the leading edge for the alloy components is due to the transferred UHMWPE film. The thickness to account for the setback is 180 nm or 1800 Å (specific gravity of UHMWPE taken as 0.94 and composition as CH_2). This thickness seems compatible with the thickness as determined from the profilometer trace across the wear track (Fig. 3). The ion beam diameter is about the same as the width of the whole wear track, so the beam analysis provides effectively an average measurement. The carbon yield represents a combination of effects. It is greater than Rutherford because of resonance scattering. It is also less than it otherwise would be because of loss of resonance due to thickness and because of inelastic scattering due to hydrogen in the polymer, but the more important of the two effects is reduction of scattering cross section due to the thickness of the film itself. This is a rather sharp resonance. The reference curve for the setback is again the same data as the curve shown in Fig. 4. To summarize, the transfer film, as detected by the RBS analysis, is compatible with profilometer results, clearly establishing that the level of polymer wear for the non-coated case to compare with the coated sample case to be discussed next.

In Fig. 7 there are two curves, although they are hardly resolvable. One is the RBS histogram a boron-coated sample (in this case the same as in Fig. 5). The other is from the same boron-coated sample but after the wear test of Fig. 3 and taken where the wear track should be. Clearly, there is no detectable difference. There is no evidence of any polymer film transfer, consistent with the profilometry results (Fig. 3). Furthermore, there is no evidence of thinning of the boron coating, i.e. no loss of boron or its oxide to the polymer or to the saline solution.

In Fig. 8, SAM images are shown for one of these coatings after sliding the 52100 bearing steel ball for about 1 h in reciprocating motion against the coated sample and under a 10 N load. As mentioned, the SAM was operated at 400 MHz. The images show some light wear on the coating, but a total absence of any voids created under the coating. Similar results were obtained with a 2 N load, except that there also was no detectable wear of the coating in that case. The SAM images of Fig. 8, correspond to different depths: (a) the surface of the coating, (b) subsurface layer $z=0$–2 μm, and (c) subsurface layer $z=2$–4 μm. The only features appearing in the SAM images are the familiar mesas due to the carbide structures and the black dots that are likely surface pits from the pre-deposition surface polishing (as determined from SEM analysis of the as-received, pre-polished, non-coated substrate). Note that these dots also appear on Fig. 1.

This test result constitutes a significant demonstration of the cohesion (or mechanical stability) and of the adhesion of these thin boron coatings to the polished Co–Cr–Mo substrate surface. Recalling the discussion at the end of Section 3.1, for the lowest measured modulus in the system (193 GPa) and the modulus of 52100 steel (the material of the steel ball), the contact area was calculated to correspond to a diameter of ~80 μm. The contact stress was 400 MPa and the Hertzian stress was 580 GPa. The importance of moving the ball is that rather than keep the Hertzian stress at below the surface, the moving ball pushes or piles up the compressive Hertzian stress out in front of the moving ball, moving it to the surface. (The idea is somewhat like pushing up a loop in a rug, which can then move out to the edge). If there was an adhesion problem for this coating, this would clearly be a certain way to cause a delamination. As mentioned, the coating did not delaminate and the acoustic microscopy showed no evidence of any tendency toward delamination.

4. Discussion

The experimental results broadly divide themselves into two important parts, but ones that are inter-connected:

The first is the wear results. The reduction in wear of the UHMWPE wear partner of the boron treated alloy is proven by the profilometer results and by the RBS results for coated and uncoated material. Collaterally, there is no sign of thinning or wear of the boron layer itself, a result that is indicated by the

profilometry and proven by RBS. With respect to the wear mechanisms discussed in the Introduction, we can only speculate in a general way as to why the boron coating is effective. First, we recall that the wear mechanisms, whatever they are, seem to work by extracting submicron polymer spheres and fibrils whose structure is somewhat intrinsic to the structure of the UHMWPE. Whether this removal process could be snagging by the fairly sharp up-thrusting carbides or adhesion due to some other factor, has not been established. The proposed idea of the rounding off and filling in with fillets of the carbide edges due to the coating could not be proven or disproven with the resolution of the topography instruments available. In other words, within resolution, the topography appeared broadly the same for the coated and uncoated samples.

It is interesting that the thickness of the adherent polymer transfer-layer (approximately 180 nm) is roughly ten times the dimension of the up-thrusting carbides. The thickness of the UHMWPE layer could represent the approximate minimum in the size of the "modular" particles that can be released from the UHMWPE structure. In other words, the polymer layer could be a continuous single layer of such particles, and this is the minimum layer thickness that one could have after a sufficiently long wear test, no matter the mechanism of snagging particles. It is interesting that the thickness is very near to the peak dimension in the sharply peaked size distribution of UHMWPE particles reported in the literature [2].

If adhesion due to factors other than the carbides is the reason for the wear, then it might be concluded that for some reason the polymer is less adherent to the boron than to the bare alloy. One observation of potential interest in this regard is that the "bare" alloy is not really bare. Although factory polished and cleaned by the factory recommended procedure, alloy surfaces had the carbon surface layer of some 15 atomic layers in thickness. This may be a wax or emulsion agent from the polish. (Based on the known size of the RBS beam spot and the typical concentration of the carbides on the surface, one can show that the carbides would make an insignificant contribution to the C signal). It is not known, whether such a carbon surface-layer in adhesion of the polymer. Apparently this carbon could be reacted in to the boron coating and incorporated together with the other carbon delivered with the boron.

Finally, in regard to the wear results, it is noted that the RBS analyses showed no evidence of silicon (Si). Thus, the silicon carbide (SiC) polishing particles, to which Ho et al. [5] attribute significant wear of the UHMWPE by polished Co–Cr–Mo would not be an issue here. The carbide regions, shown to be very hard, as expected, by the scanning nano-indenter, can only be carbides of the Co, Cr and Mo components of the alloy.

The second significant part of the experimental findings is the strong evidence for good adhesion of the coating to the substrate as manifested by several factors. These include the stability and permanence of the coating during the UHMWPE wear and steel ball sliding tests and the lack of any sign of delamination, in the form of subsurface void formation, in the subsequent scanning acoustic microscopy. Although not mentioned before, the hardness indentations were "ductile-like" with no signs of cracking, separation, or delamination around the indents. There was a general sense of comfort in the ruggedness of the samples while handling for mounting, cleaning and examination.

It is likely that the strong adhesion to the substrate is related to the prospect of strong chemical bonding with the substrate constituents. Such bonding could be predicted by the mixing enthalpy calculations, and was expected as part of the hypothesis of the boron coating. Just as importantly, bonding would be expected by examining the binary phase diagrams of B and each alloy constituent. Formation of strong compounds is expected. The bonding transition layer of 50 nm, determined by RBS, apparently represents the combination of in-diffusion and reaction that is kinetically possible at the deposition temperature. It is encouraging that this result is resolvable by RBS. Possibly treatment at higher temperatures or lowering the deposition rate by spreading of the plume over larger targets, as will be done at the production level, will enable larger transition depths. Nevertheless, what was achieved appears totally adequate thus far.

It was mentioned, however, that deposited boron films that were thicker than about 250 nm tended to delaminate, even in polymer wear tests, in sharp contrast with the case of the thinner films. Although a detail study of the materials science behind this result is the subject of future work, there is a plausible explanation in terms of the thickness of the reacted interlayer and the oxygen content in the boron film. Beginning with the latter, some of the RBS analyses were run for the incident energy of 3.03 MeV, which provides NRES detectability of oxygen. For the boron coatings, the oxygen content was below the detectability limit, which means that the concentration of the oxygen in the coating was well below 1%.

This near-absence of oxygen in the coatings deposited on Co–Cr–Mo is in clear contrast with the up to 6% oxygen found in the similarly deposited coatings on steel samples in past studies [8]. There, the ability to produce stable, adherent coatings with much larger thickness (over 400 nm) was partly attributed to this oxygen content. It is now believed that all the incorporated oxygen came from the breakup of the native oxide on the steel substrate by the energetic boron ions that are involved in this coating process. (Since oxygen was not detectable on the Co–Cr–Mo substrate surfaces, it is supposed that the oxide layers are very thin on these surfaces). Other studies with the same deposition system showed deep (~100–200 nm) diffusion interlayers of boron in the steel substrate and this phenomenon was associated with the good adhesion of the coating in an extreme environment, such as that of molten aluminum [18]. It is possible that deeper diffusion into the substrate and some intentional incorporation of oxygen into the coating, could allow for the thicker coatings to as adherent and stable as the thinner ones. However, from an industrial production viewpoint, the fact that thin coatings appear to be adequate is a big advantage.

5. Summary and conclusions

This paper presented analysis and interpretation of wear studies of boron-coated Co–Cr–Mo/UHMWPE pairs for use in metal-on-polymer type TJA orthopedic devices. The coatings

were deposited using the vacuum arc technique and with a heated boron cathode as the only source of coating material. It was found that a thin (< ~ 200 nm) boron film, as deposited on a cast, solution annealed and then pre-polished Co–Cr–Mo disk, led to a clearly detectable reduction of the wear of a UHMWPE pin in a pin-on-disk study carried out in a saline solution. After a 24-h wear test in this environment, a substantial (about 150 nm thick) polymer transfer film layer was detected on the non-coated, control samples based on both profilometry and RBS. Such transfer film was entirely absent on the coated samples. No loss of coating was detected in the tests of the coated disks. Separate tests using a steel ball sliding against the coated samples demonstrated the robustness of the coatings. Absence of voids at the coating–substrate interface, even after these latter tests, was verified with high-frequency acoustic microscopy.

It is concluded, based on these experimental results and the analyses presented in this paper, that filtered, vacuum cathodic arc-deposited, thin boron coatings on the Co–Cr–Mo contact surface can substantially extend the life of a metal-on-polymer TJA device based on this alloy. The largest benefit would be for knee replacement devices, which use cast alloy, known to have substantially more carbide precipitates than wrought alloy.

Acknowledgements

This research was supported by NIH/NIAMS, Grant Number 1 R43 AR051262-01 (Phase I SBIR) to HY-Tech Research Corporation and by the Assistant Secretary for Energy Efficiency and Renewable Energy, Office of FreedomCAR and Vehicle Technologies, as part of the High Temperature Materials Laboratory User Program at the Oak Ridge National Laboratory (ORNL), managed by UT-Battelle, LLC, for the U. S. Department of Energy under contract number DE-AC05-00OR22725. The mechanical and wear studies were carried out at ORNL under this latter program. The RBS analyses were carried out at Alabama A&M University's Research Institute (AAMURI™); the contributions of AAMURI's Dr. Claudiu Muntele in assisting with both the RBS setup and the handling of the data are gratefully acknowledged. The HY-Tech authors would like to thank Dr. E.J. Yadlowsky for continued support, advice and encouragement.

References

[1] J.M. Williams, L. Riester, R. Pandey, A.W. Eberhardt, Surf. Coat. Technol. 88 (1996) 132.
[2] M.D. Ries, A. Salehi, K. Widding, G. Hunter, J. Bone Jt. Surg., Am. 84 (2002) 129.
[3] H. McKellop, P. Campbell, S.H. Park, P. Grigoris, H.C. Amstutz, A. Sarmiento, The 20th Ann. Meet. Soc. Biomater., April 13–16, 1994, Boston, MA, USA, Trans. Soc. Biomater, 17, 1994, p. 198.
[4] D.P. Hoglin, R.J. Jacob, K.A. Saum, D. Pienkowski, R.R. Dorsch, H. Kahler, P.J. Nicholis, The 20th Ann. Meet. Soc. Biomater., April 13–16, 1994, Boston, MA, USA, Trans. Soc. Biomater., 17, 1994, p. 394.
[5] S.P. Ho, R.W. Carpick, T. Boland, M. LaBerge, Wear 253 (2002) 1145.
[6] S.M. Gorbatkin, R.L. Rhoades, T.Y. Tsui, W.C. Oliver, Appl. Phys. Lett. 65 (1994) 2672.
[7] C. Doughty, S.M. Gorbatkin, L.A. Berry, J. Vac. Sci. Technol., A 15 (1997) 2623.
[8] C.C. Klepper, R.C. Hazelton, E.J. Yadlowsky, E.P. Carlson, M.D. Keitz, J.M. Williams, R.A. Zuhr, D.B. Poker, J. Vac. Sci. Technol., A 20 (2002) 725.
[9] D. Music, U. Kreissig, Z. Czigany, U. Helmersson, J.M. Schneider, Appl. Phys., A 76 (2003) 269.
[10] D. Music, J.M. Schneider, V. Kugler, S. Nakao, J. Ping, M. Ostblom, L. Hultman, U. Helmersson, J. Vac. Sci. Technol., A 20 (2002) 335.
[11] D. Music, U. Kreissig, V. Chirita, J.M. Schneider, U. Helmersson, J. Appl. Phys. 93 (2003) 940.
[12] D. Music, V.M. Kugler, Z. Czigany, A. Flink, O. Werner, J.M. Schneider, L. Hultman, U. Helmersson, J. Vac. Sci. Technol., A 21 (2003) 1355.
[13] J.M. Williams, C.C. Klepper, R.C. Hazelton, M.D. Keitz, J.E. Lemons, M. Anabtawi, S. Luque, G.M. Ludtka, L. Riester, J. Qu, J.J. Truhan Jr., in: T. Sudarshan, J. Stiglich (Eds.), Surface Modification Technologies, ASM InternationalÒ, Materials Park, Ohio, USA, 2006, p. 72.
[14] A. Erdemir, G.R. Fenske, R.A. Erck, Surf. Coat. Technol. 43/44 (1990) 588.
[15] M. Pourbaix, Atlas of Electrochemical Equilibria in Aqueous Solutions, James A. Franklin Translation, Pergamon, London, 1966.
[16] M. Anabtawi, P. Beck, J. Lemons, J. Biomed. Mater. Res. B. Appl. Biomater. (2007), doi:10.1002/jbm.b.30894 Electronic publication ahead of print.
[17] J.M. Williams, C.C. Klepper, D.J. Chivers, R.C. Hazelton, J.J. Moschella, M.D. Keitz, in: K.J. Kirkby, R. Gwilliam, A. Smith, D. Chivers (Eds.), Ion Implantation Technology, American Institute of Physics Conference Proceedings 866, 2006, p. 261.
[18] G.M. Ludtka, V.K. Sikka, J.M. Williams, C.C. Klepper, R.C. Hazelton, E. J. Yadlowsky, 47th Annual Technical Conference Proceedings, Society of Vacuum Coaters, April 24–29, 2004, Dallas, TX, USA, 2004, p. 42.
[19] W.-K. Chu, J.W. Mayer, M.-A. Nicolet, Backscattering Spectrometry, Academic Press, New York, NY, 1978.
[20] L.R. Doolittle, Ph. D. Thesis, Cornell University, Ithaca, NY, USA, 1987.
[21] R.L. Boxman, S. Goldsmith, Surf. Coat. Technol. 52 (1992) 39.
[22] A. Anders, Surf. Coat. Technol. 120/121 (1999) 319.
[23] M. Turell, A. Wang, A. Bellare, Wear 255 (2003) 1034.
[24] M.R. Gevaert, M. LaBerge, J.M. Gordon, J.D. DesJardins, J. Tribol. 127 (2005) 740.
[25] M.A. Hamilton, M.C. Sucec, B.J. Fregly, S.A. Banks, W.G. Sawyer, J. Tribol. 127 (2005) 280.